

Performance assessment of grid-forming converters frequency support during disturbances in active distribution networks

Souhil Drias* , Abderrahmane Berkani , Mohamed Bey ,
Sarah Bouradi 

Energy Engineering and Computer Engineering Laboratory L2GEGI, Ibn Khaldoun University of Tiaret, Algeria.

*Corresponding author: souhil.drias@univ-tiaret.dz

Original Research

Received:
6 September 2024
Revised:
11 December 2024
Accepted:
20 December 2024
Published online:
1 March 2025

© 2025 The Author(s). Published by the OICC Press under the terms of the [Creative Commons Attribution License](https://creativecommons.org/licenses/by/4.0/), which permits use, distribution and reproduction in any medium, provided the original work is properly cited.

Abstract:

The use of Grid Forming Methodology (GFM) in grid-connected systems represents an innovative approach to improving the stability and flexibility of power grids. This article will elucidate the methodology, assess its frequency-related performance and stability under disturbances like load changes, and emphasize the importance of the droop control coefficient. Based on the frequency derivative, which gives more information compared to the frequency, we used the rate of change of frequency (RoCoF) instead of frequency as an indicator to compare different scenarios and highlight differences in performance after changes in loads. The RoCoF factor and the critical clearing time are determined as metrics to compare system performance and stability. To determine the gain of the controller, the Result adaptive PID controller is performed, and its performance is compared to the classical PID controller based on the trial/error method. In the rest of the article, we relied on controlling the RAPID controller, which gave the best performance. Finally, the effectiveness and accuracy of the method were verified through simulation.

Keywords: Grid forming; Droop control; Result-adaptive PID controller; Rate of change of frequency

1. Introduction

With the increasing incorporation of renewable energies into power grids, it is becoming increasingly essential to develop technologies that allow these intermittent energy sources to play an active role in balancing the grid; on the other hand, when demand for electricity increases, so does the load on the power grid [1, 2]. This increase in load can lead to a temporary drop in power system frequency. To maintain system stability, grid operators and power plants implement automatic generation control to adjust electricity production in real time in response to load variations, ensuring that frequency remains within acceptable limits. To solve this problem, inverter-based power conversion systems can use the Grid-Forming control method to maintain grid stability [5]. The control of a Grid-Forming (GFM) converter is crucial for ensuring the stability and reliability of the electrical grid; the Grid-Forming control method offers several advantages over traditional control methods. Firstly, it is more robust to load variations. Indeed, each VSC can

maintain grid voltage and frequency even if the load varies. Secondly, it enables renewable energy sources (RES) to be better integrated and connected to the grid without sophisticated control systems. The main objective of grid forming is maintaining constant voltage and frequency on the power grid, even when the load varies. In [6] Extensive, research has been conducted on the performance of Grid-Forming inverters [7]. Grid-Forming inverters are expected to be an alternative to synchronous generators for providing ancillary services in future power systems. [7] Research has also evaluated the performance of Grid-Forming inverters under balanced and unbalanced voltage phase angle jump conditions, aiming to fill the knowledge gap by providing a system view of Grid-Forming inverter-based resource controls and their impact. Although grid-tied inverters (GFMI) can potentially improve power system flexibility and reliability, some challenges and gaps still need to be addressed, such as Coordination, control methods, performance analysis, and stability. Ongoing research aims to address and

further advance the understanding and application of Grid-Forming technologies in energy systems. The controller maintains stability when switching between the two modes for inverters that connect to and generate the power grid. PID controllers play a vital role in maintaining stable voltage and current levels; classical PID controllers based on trial/error techniques may struggle with sinusoidal reference signals and disturbances, leading to performance issues. On the other hand, result in adaptive PID controllers (RAPID) offer enhanced adaptability to system changes and disturbances, leading to improved control performance [8]. This study is based on the analysis of the Rate of Change of Frequency factor (RoCoF), an important quantity that qualifies as the robustness of an electrical grid. It is the time derivative of the grid frequency and is an important quantity for evaluating the grid's robustness [9]. Load fluctuations can cause network power imbalance, resulting in changes in frequency and ROCOF [10].

In this article, we seek to improve network performance by analyzing frequency stability in the presence of some changes in load. The organization of this paper is as follows: the second section presents the method of controlling the Grid Forming some control methods and talks about the most important parameter, which is the frequency change rate. The third section discusses simulation results, the frequency dynamic performance, and the ROCOF case with load variation, and section four is dedicated to the conclusions.

2. Grid forming converter control method

Grid-Forming converter control refers to the methods and techniques used to control the operation of Grid-Forming

converters, which are power electronics devices that interface renewable energy sources (RES) such as wind and solar with the power grid [11, 12]. The control strategy must ensure that the converter operates stably and maintains the correct voltage and frequency levels required by the grid [13]. This involves designing control algorithms that regulate the converter's output power and voltage, as well as its reactive power and phase angle [10, 14]. The control system must also be able to respond quickly to changes in the grid conditions, such as variations in load and RES output [3, 12, 15]; these control methods fall into three categories figure 1.

Grid-Forming inverter (GFMI) control methodologies are a set of control algorithms that enable inverter-based distributed energy resources (DERs) to provide grid-supporting functions, such as voltage regulation and frequency stabilization. Table 1 outlines the benefits and drawbacks of GFMI control methodologies.

2.1 Droop control

Droop control is the most studied method commonly used in Grid-Forming inverters [26]. The output frequency of the inverter is adjusted according to the difference between the measured grid frequency f and a reference frequency f_0 [27, 28]. The reference frequency is usually set to the nominal grid frequency, and the inverter output frequency is adjusted according to a droop gain, a constant value set by the system operator [29–32]. This control method allows the inverter to respond to load variations and maintain grid stability [33]. The droop controllers P - f and Q - V are described in

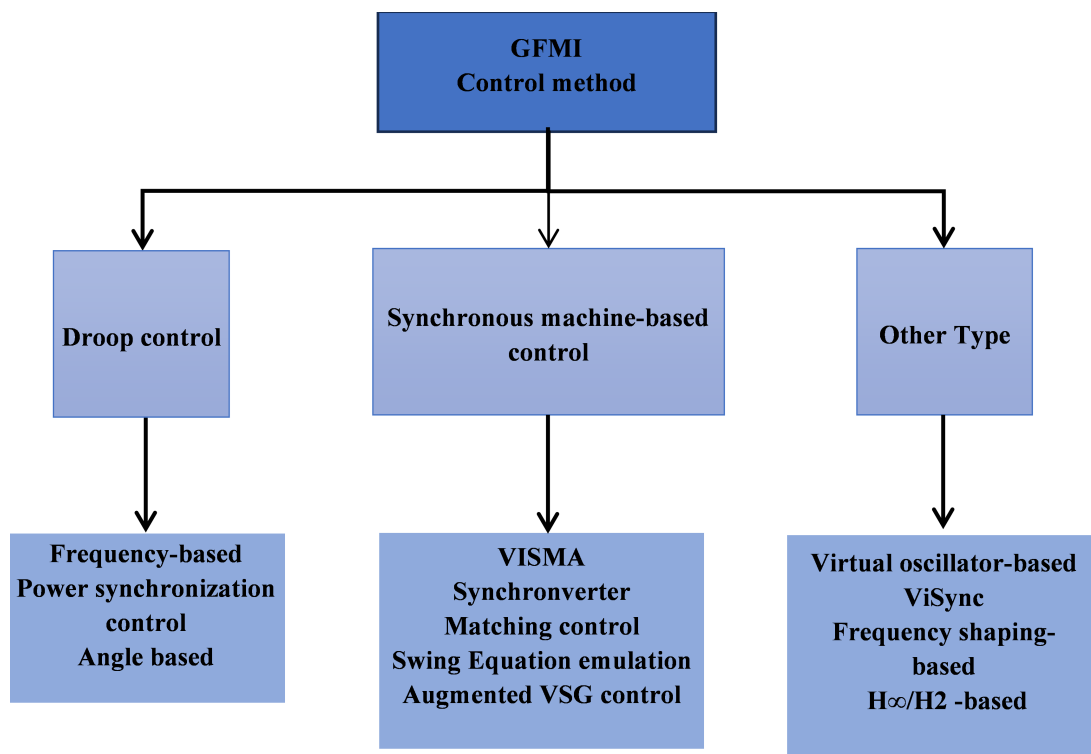


Figure 1. Grid-Forming control methodologies [3, 4].

Table 1. Advantages and disadvantages of GFM converter control methodologies.

Control Methodology	Description	Advantages	Disadvantages
Droop Control [4, 16]	A control strategy that adjusts the output power of inverters based on frequency or voltage deviations from a reference value.	Simple and decentralized control scheme. Allows for power sharing among multiple inverters without centralized communication.	Voltage deviations and power imbalances in multi-inverter systems. Limited frequency regulation capabilities.
Virtual Synchronous Generator (VSG) [17, 18]	A control technique that emulates the behaviour of a synchronous generator in an inverter-based power system.	Mimics the inertia and voltage regulation capabilities of synchronous generators. Supports stable operation and synchronization with the grid.	Requires accurate estimation of grid parameters for effective operation. May have challenges in handling dynamic disturbances and frequency deviations.
Dispatchable Virtual Oscillator Control (dVoC) [19–21]	A control approach that uses virtual oscillators to regulate the frequency and voltage of inverters, enabling them to behave like synchronous generators.	Provides frequency and voltage regulation similar to synchronous generators. Can handle grid disturbances and transitions smoothly.	Requires accurate modelling and parameter tuning for proper performance. Coordination among multiple inverters may be complex.
Virtual Oscillator Control (VoC) [22–24]	A control methodology that uses virtual oscillators to emulate inertia and damping characteristics, enabling inverters to respond to system disturbances.	Offers inertia emulation and damping capabilities. Supports grid stability during dynamic events.	Requires accurate estimation of grid parameters and model tuning. Challenges in maintaining voltage stability during large disturbances.
Matching Control (MC) [24, 25]	A control strategy that adjusts the active and reactive power outputs of inverters to match the operating characteristics of synchronous generators.	Allows for accurate synchronization with the grid. Supports stable operation and grid compatibility.	Requires precise parameter estimation and control tuning. Limited ability to handle dynamic events and frequency deviations.

equation (1)

$$\begin{cases} \omega = \omega_{ref} - k_p(P - P_{ref}) \\ V = V_{ref} - k_q(Q - Q_{ref}) \end{cases} \quad (1)$$

where V and ω are the amplitude of the output voltage and frequency of the inverter, k_p and k_q (defined as positive) represent active and reactive power drop coefficients, and the reference inputs ω_{ref} and V_{ref} are the nominal frequency and nominal voltage. P and Q are the measured VSC active and reactive power after passing through a Low-Pass filter (see figure 3). P_{ref} is the active power reference, and Q_{ref} is the reactive power reference. The coefficients k_p and k_q can be computed utilizing the following relationships:

$$\begin{cases} k_p = \frac{\Delta f}{\Delta P} = \frac{f_{max} - f_{min}}{P_{max}} \\ k_q = \frac{\Delta V}{\Delta Q} = \frac{V_{max} - V_{min}}{Q_{max}} \end{cases} \quad (2)$$

For the design of these gains k_p and k_q , we considered 5% of maximum frequency variation and 10% of maximum

voltage variation for the maximum load variation.

Where V_q and V_d are the dq constituents of the AC grid voltage, while i_d , i_q are dq constituents of the current, this operation can be realized by employing Low-Pass filters (LPF) with a reduced bandwidth. Figure 3 shows the droop control diagram block. The Low-Pass filter block is used in power calculation blocks to eliminate high-frequency noise or transients in the power signal and to provide a stable and accurate measurement of power consumption; the transfer function for a first-order Low-Pass filter is:

$$\omega_{LPF}(s) = \frac{\omega_c}{s + \omega_c} \quad (3)$$

where ω_c is the cut-off frequency of Low-Pass filters, the filtered active and reactive power is given below:

$$\begin{cases} P = \frac{\omega_c}{\omega_c + s} P \\ Q = \frac{\omega_c}{\omega_c + s} Q \end{cases} \quad (4)$$

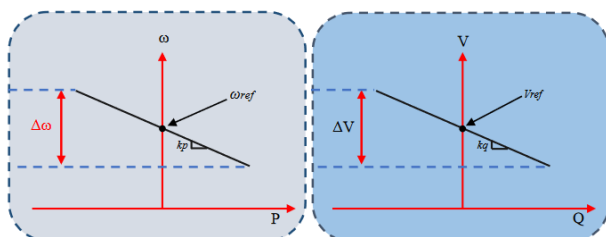


Figure 2. Droop control strategies f - P and V - Q .

3. Current and voltage controller

3.1 Proportional-Integral controller (PI)

Figure 4 depicts the cascaded control technique employed for the Voltage Source Converter (VSC). Both current and voltage serve crucial roles in Grid-Forming controllers. The current signal measures the power injected into the grid, whereas the voltage signal regulates the grid voltage. The proportional–integral controller (PI) generated the reference

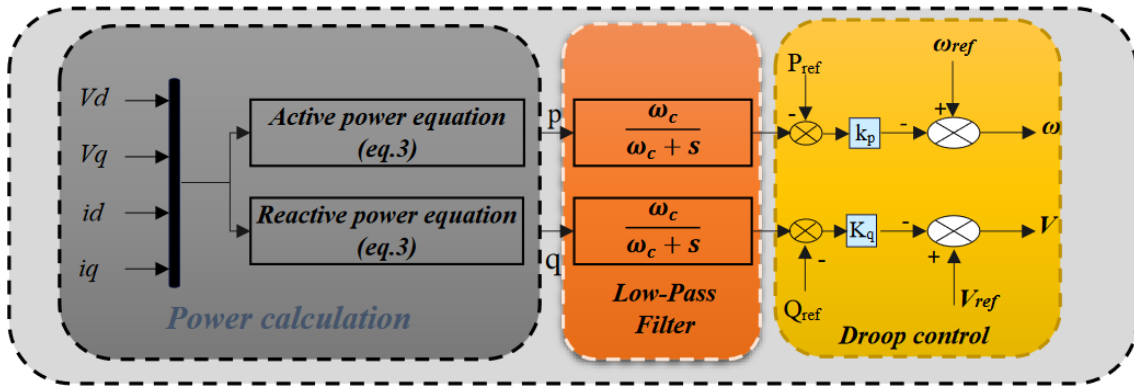


Figure 3. Droop control block diagram .

current voltage.

$$\begin{cases} i_d^* = (v_d^* - v_d) \left(k_{pv} + \frac{k_{iv}}{s} \right) + i_d - C_f \cdot \omega \cdot v_q \\ i_q^* = (v_q^* - v_q) \left(k_{pv} + \frac{k_{iv}}{s} \right) + i_q + C_f \cdot \omega \cdot v_d \end{cases} \quad (5)$$

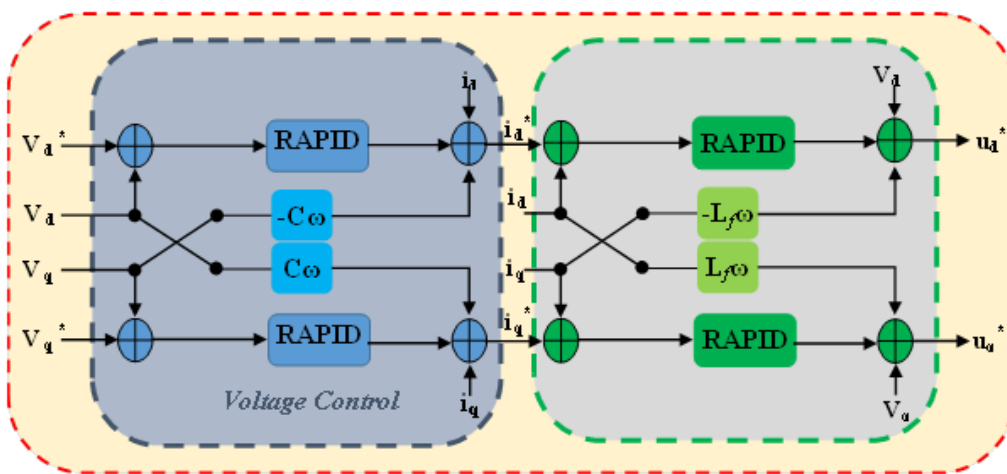
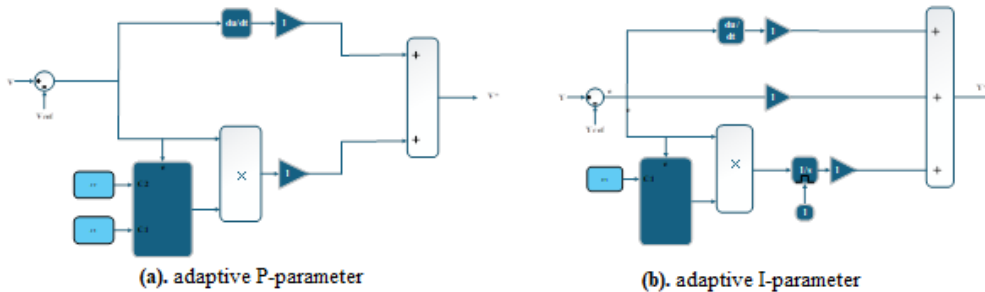
where k_{pv} and k_{iv} are the proportional and integral gains of the voltage PI controller, C_f represents the filter capacitance. Similarly, a conventional Proportional-integral (PI) current controller determines the voltage across the filter inductor. The dynamics are expressed by:

$$\begin{cases} u_d^* = (i_d^* - i_d) \left(k_{pi} + \frac{k_{ii}}{s} \right) + v_d - L_f \cdot \omega \cdot i_q \\ u_q^* = (i_q^* - i_q) \left(k_{pi} + \frac{k_{ii}}{s} \right) + v_q + L_f \cdot \omega \cdot i_d \end{cases} \quad (6)$$

k_{pi} and k_{ii} are the proportional and integral gains of the current PI controller, and L_f is the filter inductor.

3.2 Result-adaptive PID (RAPID) control

Result-adaptive PID control (RAPID control), initially developed for position control of laser scanners by M. Lugmair et al. [34], has shown significant performance improvements through experimental validation and has gained popularity thanks to its ability to adjust control parameters dynamically. Building on these positive results, RAPID control is now being considered for improving energy management in smart grids. This decision is supported by substantial experimental results from applying the laser scanner, which indicates its potential to optimize energy management



(c). The low-level cascaded control.

Figure 4. Block diagram.

in smart grids by offering greater precision and adaptability.

A. Proportional term Adaptation

P-Adaption, a method utilized in control systems, dynamically adjusts the proportional gain of a control loop based on the magnitude of the error signal. Typically, a higher proportional gain leads to faster and more precise output value correction. However, excessive gain can result in overshooting and oscillations. P-Adaption addresses this by modifying the proportional gain according to the current error value. This adjustment ensures that the gain is higher for minor errors, promoting faster convergence while reducing it for more significant errors to prevent overshoot. The adaption function, controlled by parameters c_1 and c_2 , determines the behaviour of this adjustment. The control system can optimize performance by fine-tuning these parameters, achieving high accuracy and minimal overshoot. The adaptive function of the proportional term is given by:

$$f_p(e) = 1 + \frac{c_1 - 1}{(c_2 e)^2 + 1} \tag{7}$$

Based on experimental tests conducted in [ref], for the Proportional Function, the parameter c_1 directly influences the function’s value when $e = 0$, while c_2 determines the steepness of the function. When the error values are large, the functional value approaches 1, indicating that the P-value remains unchanged. In contrast, for small values of e , the functional value equals c_1 , which signifies an increase in the P-value by a factor of c_1 .

B. Integral term Adaption

I-Adaption, another method in control systems, enhances the integral component of a control loop to eliminate steady-state error without sacrificing speed. Integrating the error signal over time allows the system to reach the set point accurately in steady-state conditions. However, adding integration to a proportional or proportional-derivative control can slow the system’s response. I-Adaption addresses this by selectively activating integration only for sufficiently small error values. This is achieved through a continuous adaption function that controls the behaviour of the integral component. Parameter c_1 determines the steepness of this function, which influences when integration is activated. During the settling phase, the adaption function suppresses integration to prevent overshoot. Once the error becomes small, integration gradually ramps up, effectively reducing residual error without causing an overshoot. By adjusting the parameter c_1 , the control system can fine-tune the behaviour of the adaption function, optimizing performance and achieving precise control without sacrificing speed. The adaptive function of the proportional term is given by:

$$f_i(e) = \frac{1}{(c_1 e)^2 + 1} \tag{8}$$

For the Integrator Function: Here, only the parameter c_1 needs to be set, which dictates the function’s steepness. The function’s value approaches zero for large error values, while for minor errors, it approaches one. The integral component of the control is multiplied by the functional

value of the adaptive function, represented by c_1 . As a result, during the settling phase-when the error value is significant-the integrator input is clamped to zero. Only after the error value decreases (post-settling) are the input released. This approach ensures that the integration of the error and the reduction of the error commence only after the settling phase, effectively preventing any overshoot.

4. The Rate of Change of Frequency (RoCoF)

The Rate of Change of Frequency (RoCoF) indicates the power system frequency’s change over time, measured by the derivative of frequency (df/dt) [29]. RoCoF is a critical parameter in power system stability, allowing ongoing monitoring of system performance and behaviour during disruptions and contingencies. The prevalent frequency standards are 50 Hz or 60 Hz in North America. Detecting RoCoF is essential to maintaining power grid stability and preventing possible blackouts, requiring continuous monitoring and control of RoCoF values to avert a system breakdown. In other words, ROCOF represents how quickly grid frequency changes in response to rapid load changes. The RoCoF can be calculated in the following way:

$$\text{RoCoF}_T = \frac{df}{dt} = \frac{f_T - f_0}{T} \tag{9}$$

5. Virtual impedance technique

The virtual impedance technique is commonly used in micro grids with highly resistive elements to achieve active and reactive power regulation. By introducing virtual impedance, it is possible to compensate for the mismatched line impedances and improve power control accuracy by incorporating extra information from the point of common coupling (PCC) [36, 37]. A fixed virtual inductance is typically introduced to generate the reference for reactive power,

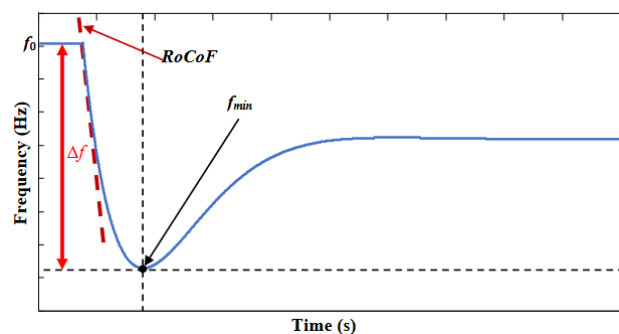


Figure 5. Frequency response of a power system.

Table 2. International grid codes for RoCoF [35].

Grid Code	ROCOF (Hz/s)	T (ms)
Germany	2 Hz/s (50 Hz)	500 ms
Ireland	1 Hz/s (50 Hz)	200 ms
UK	1 Hz/s (50 Hz)	500 ms
Denmark	2 Hz/s (50 Hz)	500 ms
Italy	2.5 Hz/s (50 Hz)	100 ms
South Africa	1.5 Hz/s (50 Hz)	only for RES
IEEE	0.4 Hz/s (60 Hz)	N.A
USA	No standard for RoCoF (60 Hz)	N.A

which is removed to recover the output voltage [38, 39]. The control block diagram of the virtual impedance is shown in the following figure 6.

Design of the VSC output filter

An LCL filter is commonly used in power electronics systems to reduce harmonics and electromagnetic interference (EMI) generated by power converters, such as inverters or rectifiers. The name “LCL” refers to the arrangement of the filter components: an inductor (L), a capacitor (C), and another inductor (L) in series; the inductors in the LCL filter help to limit the rate of change of current, reducing the voltage spikes and harmonics generated by power converters [40]. The capacitor acts as a short circuit for high-frequency components, diverting them from the load and preventing their propagation into the power supply system [41, 42]. The LCL filter depends on system parameters such as nominal power and DC bus voltage V_{dc} , switching frequency f_c , modulation ratio, voltage, and network frequency. It exacts other factors like the cost factor. The Following equations represent the LCL filter parameters:

a. Capacitance C

$$C = \frac{0.05}{\omega_n Z_{base}} \tag{10}$$

$$Z_{base} = \frac{V_{L-L}^2}{S_n} \tag{11}$$

$$C = 0.05 \frac{S_n}{2\pi f_g V_{L-L}^2} \tag{12}$$

V_{L-L} is the RMS Line-Line output of the inverter, S_n is the rated active power of the inverter, f_g is the grid frequency, and ω_n is the inverter switching frequency.

b. L_1 inductance on the inverter side

$$L_1 = \frac{V_s}{2\sqrt{6}f_s i_{lim} \times 0.15} \tag{13}$$

c. L_2 inverter side inductance

$$L_2 = L_1 \tag{14}$$

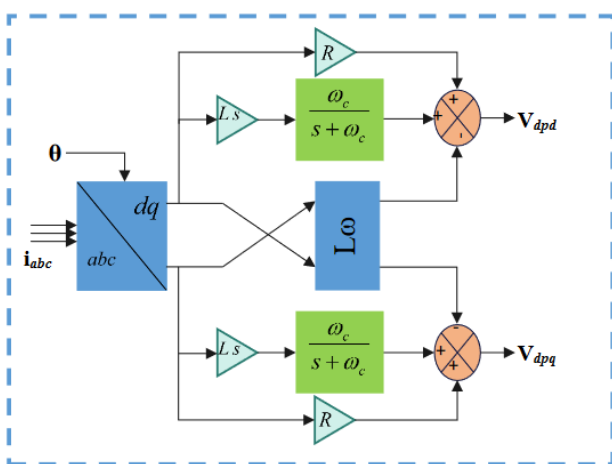


Figure 6. Block diagram of the virtual impedance loop.

6. Simulation results

Figure 7 shows the complete dynamic model of the primary grid with grid forming control on a 2-level VSC; the system consists of a three-phase, two-level inverter VSC fed by a DC power source VDC, the VSC connected to the infinite grid through an LCL filter. The purpose of the LCL filter is to eliminate the high-frequency harmonics caused by PWM signals. The PWM is a control method used in Grid-Forming inverters. In PWM, the width of the pulses of the output waveform is varied to control the power flow. The use of PWM in Grid-Forming control allows for precise control of the output voltage and frequency, which is necessary for maintaining the stability and integrity of the grid. It also provides for efficient power transfer and reduced power losses. The Grid-Forming control regulates the converter output voltage and frequency and then synchronizes them with the grid voltage and frequency. To validate the performed analysis, the studied system has been simulated in MATLAB/Simulink; the system included a GD (distributed generator) connected to the mains with a balanced load to evaluate the control performance studied. The inverter’s DC source is a battery with a constant value. Table 3 provides an overview of the system’s parameters.

We used the RAPID regulator presented above to ensure a robust regulator with optimal gains, thus avoiding the trial-and-error methods used in classic regulators. Figure 8 compares the voltage response in the case of a classical PID with the optimal gains designed by the RAPID regulator.

As shown in this figure (figure 8), the RAPID controller adjusts its parameters dynamically based on system behaviour, offering improved performance in scenarios where traditional PID control may struggle to optimize performance.

Table 5 summarizes the comparison of the critical parameters in the two cases. Based on these results, we can see that in the cases of rise time, maximum peak overshoot, and steady-state error, the RAPID controller always has better performance, while the traditional PI controller has poor tracking performance. The RAPID controller is used in the

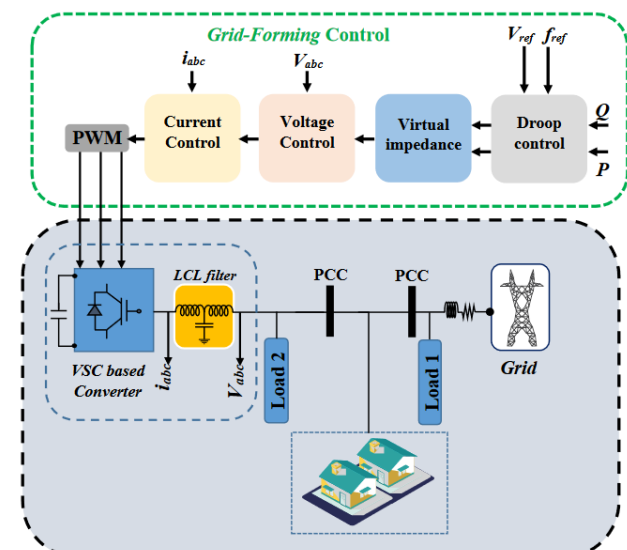


Figure 7. Complete control of a VSC-PWM using cascaded loops.

Table 3. System parameters.

	Description	Symbol	Value
VSC (GFM)	Nominal line-line Voltage	V_{LL}	380 v
	Nominal angular frequency	ω_n	$2.\pi.50$ rd/s
	DC link voltage	V_{dc}	700 V
	Switching frequency	f_s	10 KHz
	Inverter output inductance	L_f	0.0042 H
	Inverter output capacitance	C_f	40 μ F
	Power active reference	P_{ref}	15 KW
	Active power droop gain	K_p	5.10^{-4}
	Reactive power droop gain	K_q	0.002
	cut-off frequency of LPF	ω_c	12.57 rd/s
Grid	Grid voltage	V_g	220 V
	Grid Frequency	f_g	50 Hz
	Grid inductance	L_g	16.58 mH
	Grid Resistance	R_g	0.893 Ω
Load	Active power	P_1, P_2	12 KW, 10 KW
	Reactive power	Q_1, Q_2	200 Var , 1 KVar

rest of the simulation.

The proposed system depicted in figure 7 underwent simulation analysis to assess its performance. At time $t = 2$ seconds, the load changed. The scenarios were chosen to test the operation of the grid forming control. In cases of load increase, the load is assumed to be a PQ load, and we control the output voltage and frequency in the load and active power of the grid and VSC. Figures 9 to 12 display the voltage and current waveforms of the VSC before and after the filter.

Table 4. Gains of PI and RAPID.

PI	RAPID
$K_p = 0.286$	$K_p = 0.7700$
$K_i = 600$	$K_i = 8.9442$

Before $t = 2$ sec, the active power demand is 22 kW, the grid's power is 7 kW, and P_{scv} is 15 kW. This achieves equal demand and production ($P_g = P_{load}$). Figures 13 to 15 present the active and reactive power. The results confirm that the suggested controller offers a solution to tackle the challenge of achieving power distribution and ensuring stable performance in VSC. As the load varies, the voltage remains constant and sinusoidal ($V_{rms} = 220$ V), and the inverter reacts quickly to the increase in load compared with

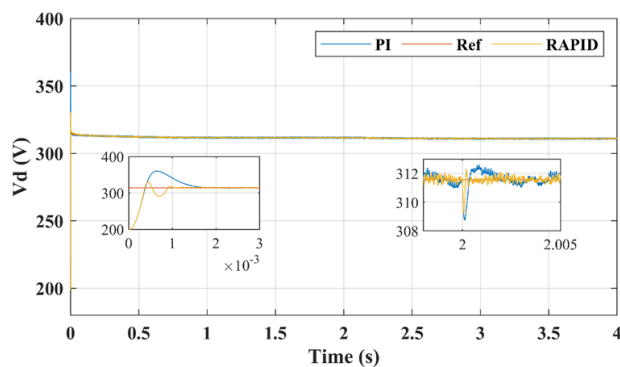


Figure 8. Voltage loop response, comparison between PI and RAPID controller.

the mains.

This section, analyses the system's frequency and power response to the control parameters. The K_p value chosen in this simulation is between 1.25×10^{-4} and 5×10^{-4} .

Since RoCoF is usually evaluated using several different time frames, in this case, It is used with a time window of 150 ms; Table 5 shows the RoCoF and frequency nadirs measured for different K_p values.

The droop control coefficient variation can influence the power system's performance. If the coefficient is set too low, the frequency may take too long to adjust to changes in the load. VSCs use droop control to regulate their output power based on the grid frequency. This ensures that the VSCs provide power in proportion to the grid demand, which helps stabilize the grid during high or low supply times. The variation of the droop control coefficient can significantly affect the performance of the VSC system. The droop control coefficient is directly proportional to the rate of change of frequency and voltage of the VSC, which affects the stability and dynamic response of the system. The variation of K_p in droop control affects the stability of the system. A higher K_p value will result in a faster response of the system to changes in load, but it may also make the system more unstable. A lower K_p value will result in a slower system response but may be more stable. When load variations occur, Grid-Forming inverters can adjust their output power to compensate for the changes. This helps maintain the grid's stability and ensure that all loads are supplied with power.

Increasing the droop control coefficient can help reduce the rate of change of frequency (RoCoF) during conditions, thereby enhancing the power system's stability. However, using a high droop control coefficient may result in frequency deviations and oscillations, posing a risk to the system's overall stability.

In this section, we analyze the system's frequency and power response about the control parameters. The K_p value chosen in this simulation is 2.51×10^{-4} with variations in load (10%, 20% and 30%).

A key aspect of power system dynamics is the relationship

Table 5. Performance comparison of controllers.

Controllers	Performance indices	0 – 2 s	2 – 4 s
PI Controllers	Rise time (tr)	1.655 ms	0.5 ms
	Maximum peak overshoot (%Mp)	15.75	0.4
	Steady state error (ess)	0.35	0.28
Result-adaptive PID Controller	Rise time (tr)	1.12 ms	0.2 ms
	Maximum peak overshoot (%Mp)	4.5	0.24
	Steady state error (ess)	0.25	0.19

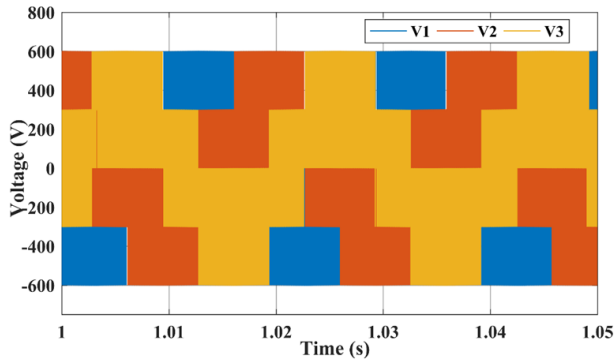


Figure 9. Voltage waveforms of the three-phase inverter (before filter).

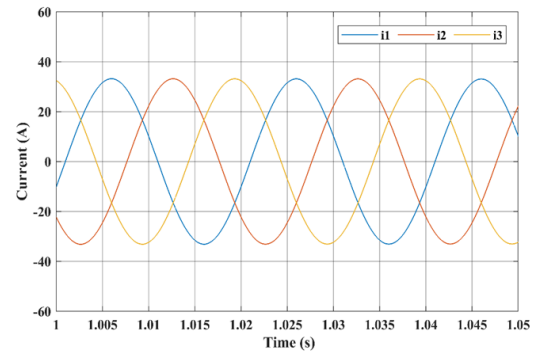


Figure 12. Current waveforms of the three-phase inverter (after filter).

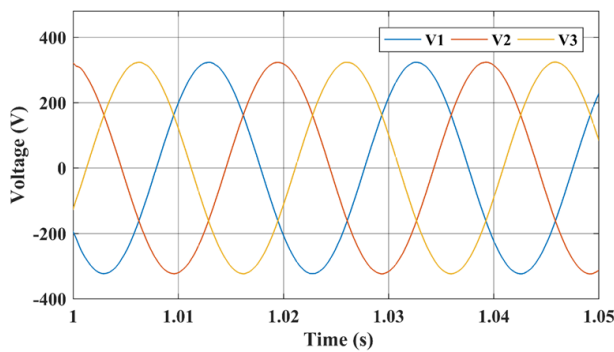


Figure 10. Voltage waveforms of the three-phase inverter (after filter).

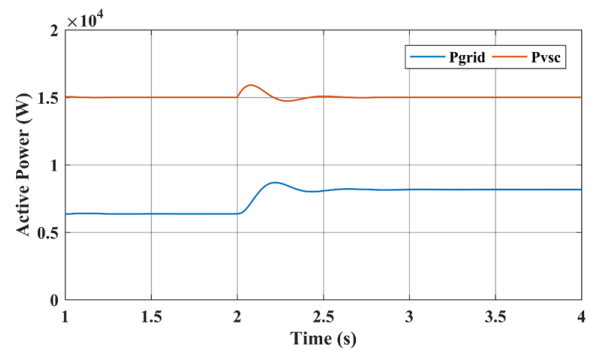


Figure 13. Active grid power and VSC with load variation.

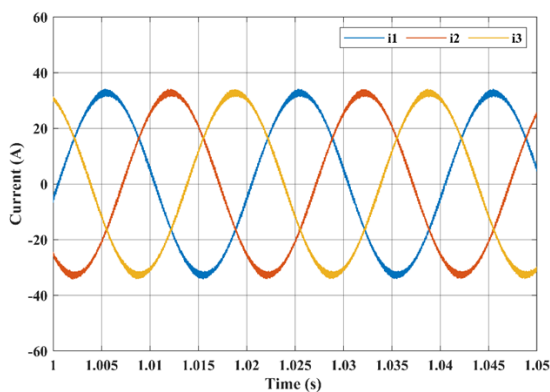


Figure 11. Current waveforms of the three-phase inverter (before filter).

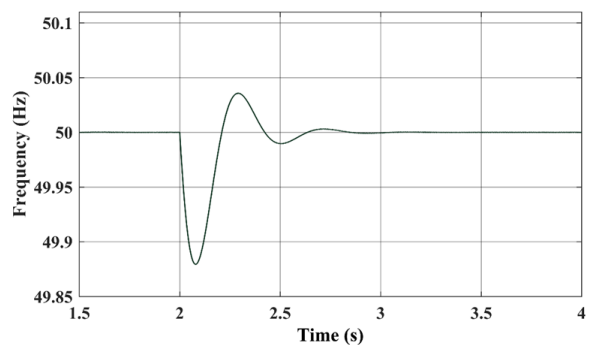


Figure 14. Frequency response curve.

between an increase in power and frequency. When power increases, the power system’s frequency tends to decrease, and RoCoF measures the rate of this frequency change. The following table represents the frequency measurement with load variations. Variations in RoCoF as a function of load changes can im-

pact system performance. From Table 7, we conclude that as the load increases, the frequency decreases. This proves that the methodology ($f-p$ droop control) is correct; the higher the load, the higher the RoCoF. Although the load reached 30%, the RoCoF values are still within internationally accepted values < 1 Hz/s; this proves the Performance of Grid Forming control.

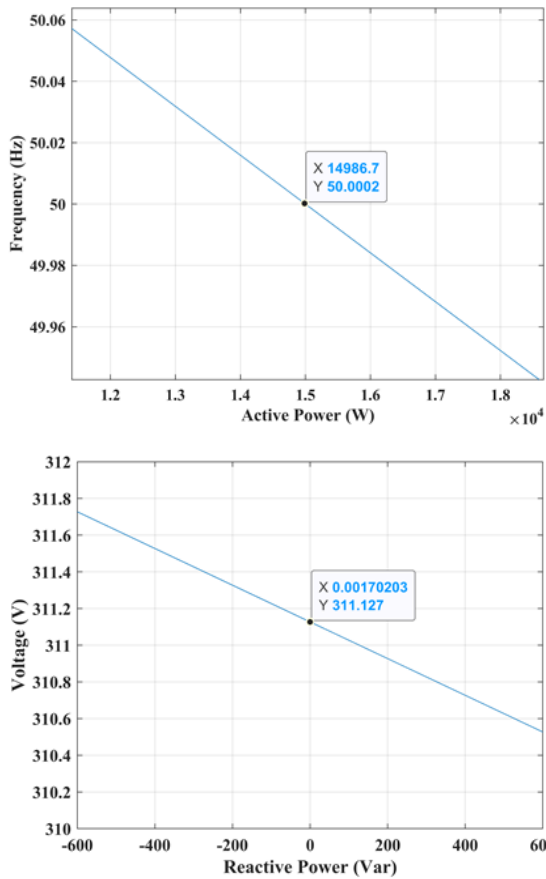


Figure 15. The resultant P - f and Q - V droops.

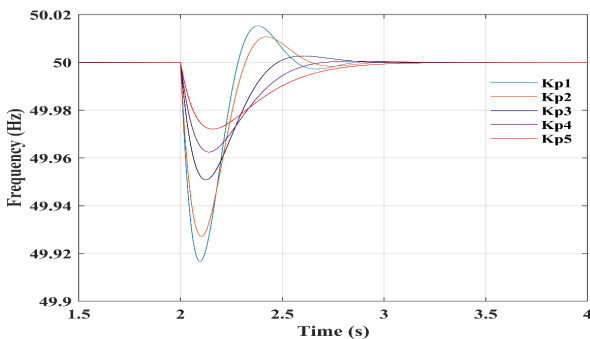


Figure 16. Comparison between frequency responses for different K_p values.

7. Conclusion

This article is interested in the Grid-Forming converter technique applied in micro-networks. Therefore, we have evaluated its power to restore the network to a stable state after it is subjected to a slight movement disturbance represented by the variation dump. To identify the gains of regulators, we have chosen to use a new adaptive regulator; the latter has practically confirmed its performance, which is validated in our case, where we have proven its power has imposed reasonable gains. Finally, to evaluate the performances obtained by our method used in the event of a load variation, thus the capacity of the adaptive regulator used, the ReCof is used as an evaluation index because of its importance in studies of the behaviour of

Table 6. RoCoF and fall frequency for different K_p values (For the case studies in this research, $T = 0.15s$ is used).

K_p	RoCoF (Hz/s)	Fall frequency (Nadir) (Hz)
$K_{p1} = 5.00 \times 10^{-4}$	0.460	49.91
$K_{p2} = 4.18 \times 10^{-4}$	0.453	49.93
$K_{p3} = 2.51 \times 10^{-4}$	0.340	49.95
$K_{p4} = 1.79 \times 10^{-4}$	0.260	49.96
$K_{p5} = 1.25 \times 10^{-4}$	0.200	49.97

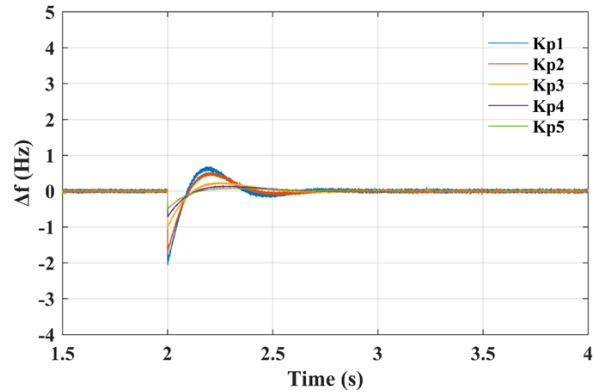


Figure 17. Frequency deviation of different K_p values.

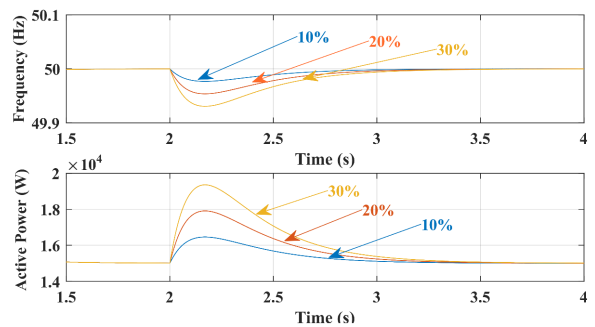


Figure 18. Comparison between frequency responses and active power for load variation.

micro-networks, the analysis of this factor through different simulations allowed us to confirm the capacity of the GFI control thus ensuring the improvement of its performance using a RAPID controller.

Table 7. RoCoF and fall Frequency of 10% to 30% total load disturbance.

Load Variation	RoCoF (Hz/s)	Fall frequency (Nadir) (Hz)
10%	0.34	49.95
20%	0.67	49.90
30%	0.94	49.86

Authors contributions

Authors have contributed equally in preparing and writing the manuscript.

Availability of data and materials

The data that support the findings of this study are available from the corresponding author upon reasonable request.

Conflict of interests

The authors declare that they have no known competing financial interests or personal relationships that could have appeared to influence the work reported in this paper.

References

- [1] A. Narula, P. Imgart, M. Bongiorno, M. Beza, J. R. Svensson, and J. P. Hasler. “Voltage-Based Current Limitation Strategy to Preserve Grid-Forming Properties Under Severe Grid Disturbances.”. *IEEE Open Journal of Power Electronics*, 4:176–188, 2023. DOI: <https://doi.org/10.1109/OJPEL.2023.3246728>.
- [2] Z. Zhou, W. Wang, T. Lan, and G. M. Huang. “Dynamic Performance Evaluation of Grid-Following and Grid-Forming Inverters for Frequency Support in Low Inertia Transmission Grids.”. *2021 IEEE PES Innovative Smart Grid Technologies Europe (ISGT Europe), Espoo, Finland*, pages 01–05, 2021. DOI: <https://doi.org/10.1109/ISGTEurope52324.2021.9640034>.
- [3] N. Mohammed, H. H. Alhelou, and B. Bahrani. “Grid-Forming Power Inverters: Control and Applications.”. *CRC Press*, 2-23.
- [4] D. B. Rathnayake, M. Akrami, C. Phurailatpam, et al. “Grid-Forming Inverter Modeling, Control, and Applications.”. *IEEE Access*, 9:114781–114807, 2021. DOI: <https://doi.org/10.1109/ACCESS.2021.3104617>.
- [5] J. L. Rodríguez-Amendedo, S. Arnaltes Gómez, M. Zubiaga, et al. “Grid-Forming Control of Voltage Source Converters Based on the Virtual-Flux Orientation.”. *IEEE Access*, 11:10254–10274, 2023. DOI: <https://doi.org/10.1109/ACCESS.2023.3240516>.
- [6] H. Kikusato et al. “Performance analysis of grid-forming inverters in existing conformance testing.”. *Energy Reports*, 8:73–83, 2022. DOI: <https://doi.org/10.1016/j.egy.2022.10.106>.
- [7] R. Darbali-Zamora, N. S. Gurule, J. Hernandez-Alvidrez, S. Gonzalez, and M. J. Reno. “Performance of a Grid-Forming Inverter Under Balanced and Unbalanced Voltage Phase Angle Jump Conditions.”. *2021 IEEE 48th Photovoltaic Specialists Conference (PVSC), Fort Lauderdale, FL, USA*, pages 1409–1416, 2021. DOI: <https://doi.org/10.1109/PVSC43889.2021.9518539>.
- [8] L. Gutiérrez, J. Roberto, P. Ponce Cruz, and A. Molina Gutiérrez. “Bounded Region Optimization of PID Gains for Grid Forming Inverters with Genetic Algorithms.”. *Mexican International Conference on Artificial Intelligence. Cham: Springer International Publishing*, 2019. DOI: <https://doi.org/10.1007/978-3-030-33749-0-23>.
- [9] Z. Zhou, W. Wang, T. Lan, and G. M. Huang. “Dynamic Performance Evaluation of Grid-Following and Grid-Forming Inverters for Frequency Support in Low Inertia Transmission Grids.”. *2021 IEEE PES Innovative Smart Grid Technologies Europe (ISGT Europe), Espoo, Finland*, pages 01–05, 2021. DOI: <https://doi.org/10.1109/ISGTEurope52324.2021.9640034>.
- [10] D. Pan, X. Wang, F. Liu, and R. Shi. “Transient Stability of Voltage-Source Converters with Grid-Forming Control: A Design-Oriented Study.”. 2019.
- [11] O. Gomis-Bellmunt, S. D. Tavakoli, V. Albernaz Lacerda, et al. “Grid-Forming Loads: Can the loads be in charge of forming the grid in modern power systems?.”. *IEEE Transactions on Smart Grid*, 14(2):1042–1055, 2022. DOI: <https://doi.org/10.1109/TSG.2022.3202646>.
- [12] N. B. Lai. “Control of Power Converter in Modern Power Systems.”. *PhD thesis, Universitat Politècnica de Catalunya, Barcelona*, 2022.
- [13] M. Poursmaeil et al. “An Enhanced Control of Grid-forming Converters for Systems with High Penetration of Renewable Energies.”. 2022.
- [14] J. Rocabert, A. Luna, F. Blaabjerg, et al. “Control of Power Converters in AC Microgrids.”. *IEEE Transactions on Power Electronics*, 27(11):4734–4749, 2012. DOI: <https://doi.org/10.1109/TPEL.2012.2199334>.
- [15] Z. Zhou, W. Wang, T. Lan, and G. M. Huang. “Dynamic Performance Evaluation of Grid-Following and Grid-Forming Inverters for Frequency Support in Low Inertia Transmission Grids.”. *2021 IEEE PES Innovative Smart Grid Technologies Europe (ISGT Europe), Espoo, Finland*, pages 01–05, 2021. DOI: <https://doi.org/10.1109/ISGTEurope52324.2021.9640034>.
- [16] P. Unruh, M. Nuschke, P. Straub, et al. “Overview on Grid-Forming Inverter Control Methods.”. *Energies*, 13(10):2589, 2020. DOI: <https://doi.org/10.3390/en13102589>.
- [17] M. Shadoul, R. Ahshan, R. S. Alabri, et al. “A Comprehensive Review on a Virtual-Synchronous Generator: Topologies, Control Orders and Techniques, Energy Storages, and Applications.”. *Energies*, 15(22):8406, 2022. DOI: <https://doi.org/10.3390/en15228406>.
- [18] S. D’Arco and J. A. Suul. “Virtual Synchronous Machines—Classification of Implementations and Analysis of Equivalence to Droop Controllers for Microgrids.”. *IEEE*, pages 1–7, 2013. DOI: <https://doi.org/10.1109/PTC.2013.6652456>.
- [19] G. S. Seo, M. Colombino, I. Subotic, et al. “Dispatchable Virtual Oscillator Control for Decentralized Inverter-Dominated Power Systems: Analysis and Experiments.”. *IEEE*, pages 561–566, 2019. DOI: <https://doi.org/10.1109/APEC.2019.8722028>.
- [20] D. Grob, M. Colombino, J. S. Brouillon, et al. “The Effect of Transmission-Line Dynamics on Grid-Forming Dispatchable Virtual Oscillator Control.”. *IEEE Transactions on Control of Network Systems*, 6(3):1148–1160, 2019. DOI: <https://doi.org/10.1109/TCNS.2019.2921347>.
- [21] N. Mohammed, M. Ali, M. Ciobotaru, and J. Fletcher. “Accurate control of virtual oscillator-controlled islanded AC microgrids.”. *Electric Power Systems Research*, 214:108791, 2023. DOI: <https://doi.org/10.1016/j.epr.2022.108791>.
- [22] P. Unruh, M. Nuschke, P. Straub, et al. “Overview on Grid-Forming Inverter Control Methods.”. *Energies*, 13(10):2589, 2020. DOI: <https://doi.org/10.3390/en13102589>.
- [23] S. Azizi Aghdam and M. Agamy. “Virtual Oscillator-Based Methods for Grid-Forming Inverter Control: A Review.”. *IET Renewable Power Generation*, 16(5):835–855, 2022. DOI: <https://doi.org/10.1049/rpg2.12398>.
- [24] A. Tayyebi, F. Dörfler, F. Kupzog, et al. “Grid-Forming Converters - Inevitability, Control Strategies, and Challenges in Future Grids Application.”. 2018.
- [25] C. Arghir, T. Jouini, and F. Dörfler. “Grid-Forming Control for Power Converters Based on Matching of Synchronous Machines.”. *Automatica*, 95:273–282, 2018. DOI: <https://doi.org/10.1016/j.automatica.2018.05.037>.
- [26] E. Buraimoh, A. O. Aluko, O. E. Oni, et al. “Decentralized Virtual Impedance-Conventional Droop Control for Power Sharing for Inverter-Based Distributed Energy Resources of a Microgrid.”. *Energies*, 15(12):4439, 2022. DOI: <https://doi.org/10.3390/en15124439>.

- [27] J. He, Y. Liu, and Y. Wang. “Cascaded Droop and Inverse Droop Regulation for Two-Layer Coordinated Power Flow Control in Series-Connected Power Cells.”. *IEEE Transactions on Industrial Electronics*, 68(8):6939–6951, 2020. DOI: <https://doi.org/10.1109/TIE.2020.3005099>.
- [28] Q. Salem, R. Aljarrah, M. Karimi, et al. “Grid-Forming Inverter Control for Power Sharing in Microgrids Based on P/f and Q/V Droop Characteristics.”. *Sustainability*, 15(15):11712, 2023. DOI: <https://doi.org/10.3390/su151511712>.
- [29] H. Bevrani and S. Shokoochi. “An Intelligent Droop Control for Simultaneous Voltage and Frequency Regulation in Is-landed Microgrids.”. *IEEE Transactions on Smart Grid*, 4(3):1505–1513, 2013. DOI: <https://doi.org/10.1109/TSG.2013.2258947>.
- [30] N. N. Opiyo. “Droop Control Methods for PV-Based Mini Grids with Different Line Resistances and Impedances.”. *Smart Grid and Renewable Energy*, 9(6):101–112, 2018. DOI: <https://doi.org/10.4236/sgre.2018.96007>.
- [31] Z. Shuai, S. Mo, J. Wang, et al. “Droop Control Method for Load Share and Voltage Regulation in High-Voltage Microgrids.”. *Journal of Modern Power Systems and Clean Energy*, 4(1):76–86, 2016. DOI: <https://doi.org/10.1007/s40565-015-0176-1>.
- [32] A. Saleh-Ahmadi, M. Moattari, A. Gahedi, et al. “Droop Method Development for Microgrids Control Considering Higher Order Sliding Mode Control Approach and Feeder Impedance Variation.”. *Applied Sciences*, 11(3):967, 2021. DOI: <https://doi.org/10.3390/app11030967>.
- [33] S. Anttila, J. S. Döhler, J. G. Oliveira, et al. “Grid Forming Inverters: A Review of the State of the Art of Key Elements for Microgrid Operation.”. *Energies*, 15(15):5517, 2022. DOI: <https://doi.org/10.3390/en15155517>.
- [34] M. Bey, R. Araria, S. Bouradi, S. Drias, and A. Thamer. “Result-adaptive PID control based ant colony optimization tuning for battery operation control in standalone PV system with consumption side power management.”. *Electrica*, 24(3):710–721, 2024. DOI: <https://doi.org/10.5152/electrica.2024.24041>.
- [35] W. Binbing, X. Abuduwayiti, C. Yuxi, and T. Yizhi. “RoCoF Droop Control of PMSG-Based Wind Turbines for System Inertia Response Rapidly.”. *IEEE Access*, 8:181154–181162, 2020. DOI: <https://doi.org/10.1109/ACCESS.2020.3027740>.
- [36] Q. Taoufik, H. Wu, X. Wang, et al. “Variable Virtual Impedance-Based Overcurrent Protection for Grid-Forming Inverters: Small-Signal, Large-Signal Analysis, and Improvement.”. *IEEE Transactions on Smart Grid*, 2022. DOI: <https://doi.org/10.1109/TSG.2022.3232987>.
- [37] W. Deng, N. Dai, K. W. Lao, et al. “A Virtual-Impedance Droop Control for Accurate Active Power Control and Reactive Power Sharing Using Capacitive-Coupling Inverters.”. *IEEE Transactions on Industry Applications*, 56(6):6722–6733, 2020. DOI: <https://doi.org/10.1109/TIA.2020.3012934>.
- [38] E. Buraimoh and I. E. Davidson. “Fault Ride-Through Analysis of Current- and Voltage-Source Models of Grid Supporting Inverter-Based Microgrid.”. *IEEE Canadian Journal of Electrical and Computer Engineering*, 44(2):189–198, 2021. DOI: <https://doi.org/10.1109/ICJECE.2020.3035036>.
- [39] X. Lin, R. Zamora, and C. Baguley. “Droop Control Based on Improved Virtual Impedance in a Stand-Alone Microgrid.”. *IEEE*, 2019.
- [40] S. Li, X. Fu, M. Ramezani, et al. “A Novel Direct-Current Vector Control Technique for Single-Phase Inverter with L, LC and LCL Filters.”. *Electric Power Systems Research*, 125:235–244, 2015. DOI: <https://doi.org/10.1016/j.epsr.2015.04.006>.
- [41] N. Rasekh and M. Hosseinpour. “LCL Filter Design and Robust Converter Side Current Feedback Control for Grid-Connected Proton Exchange Membrane Fuel Cell System.”. *International Journal of Hydrogen Energy*, 45(23):13055–13067, 2020. DOI: <https://doi.org/10.1016/j.ijhydene.2020.02.227>.
- [42] P. Bolsi, E. Prado, C. Sartori, M. Lenz, and J. R. Pinheiro. “LCL Filter Parameter and Hardware Design Methodology for Minimum Volume Considering Capacitor Lifetimes.”. *Energies*, 15:4420, 2022. DOI: <https://doi.org/10.3390/en15124420>.